Optical properties and structures of silver thin films deposited by magnetron sputtering with different thicknesses

Xilian Sun (孙喜莲), Ruijin Hong (洪瑞金), Haihong Hou (侯海虹), Zhengxiu Fan (范正修), and Jianda Shao (邵建达)

Shanghai Institute of Optics and Fine Mechanics, Chinese Academy of Sciences, Shanghai 201800

Received January 17, 2006

A series of thin Ag films with different thicknesses grown under identical conditions are analyzed by means of spectrophotometer. From these measurements the values of refractive index and extinction coefficient are calculated. The films are deposited onto BK7 glass substrates by direct current (DC) magnetron sputtering. It is found that the optical properties of the Ag films can be affected by films thickness. Below critical thickness of 17 nm, which is the thickness at which Ag films form continuous films, the optical properties and constants vary significantly with thickness increasing and then tend to a stable value up to about 40 nm. At the same time, X-ray diffraction measurement is carried out to examine the microstructure evolution of Ag films as a function of films thickness. The relation between optical properties and microstructure is discussed.

OCIS codes: 310.0310, 160.3900, 310.6860, 120.4530, 260.3910.

Compared with other metal films, Ag films have attracted interest for years due to their adequate performances: the highest reflectivity and the lowest polarization for the full infrared (IR) region and down to a wavelength of 400 nm; a very low absorption in the visible wavelength region; stability in aqueous solutions of any PH as long as oxidizing agents or complexing substances are not present[1,2]. The optical applications are energy-efficient glass windows for warm climate[3], transparent conductive coatings[4,5], transparent heat mirror[6] and so on. Normally in order to get the optimum optical or electrical characteristics of these Ag-based compound films, a suitable thickness of Ag film is chosen in the design, calculations, and applications for multilayer stacks. In most cases, the optical constants of thin films used in these applications are obtained from bulk silver. However, the actual optical constants of the thin films may be quite different, the reason may be correlated with the structure variation[2]: silver islands nucleation on the substrate, the linking among individual islands with well separated 'island clusters', and the transition to a closed film. This change can be seen from Fig. 1. Below a certain critical thickness, thin films consist of isolated islands. Their optical constants and properties depend on the size and shape of the islands and their separation, the substrate, the deposition conditions, etc.. As the thickness increases beyond the critical value, their properties tend to a stable value. Thus the optical properties and absorption of Ag film show a series of anomalous variations with increasing film thickness. The critical thickness and the correlation between the optical properties and microstructure can be determined from measured optical constants and absorption as a function of film thickness[7].

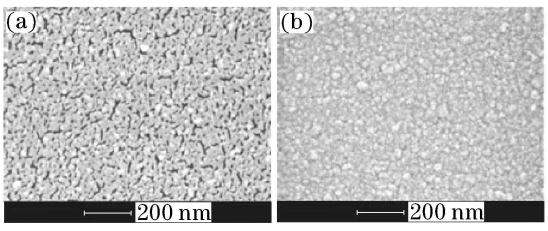

Fig. 1. Scanning electron micrographs from Ag films deposited on glass substrates. (a) Silver film with isolated islands; (b) a closed film.

Much research has been performed on Ag film[8−11], few reports have focused on the correlation between optical constants and microstructure of Ag films. This paper deals with the experimental results and a qualitative discussion of the relationship, providing a good foundation for the film design and performance analysis.

A series of Ag films with different thicknesses were prepared by direct current (DC) magnetron sputtering using an Ag target (99.99%) on BK7 glass substrates at room temperature. Before deposition, the substrates were carefully cleaned with ether solvent. The chamber was pumped to a base pressure of 1.8×10^{-3} Pa before deposition. Film growth was carried out in the growth ambient with high purity argon as working gas and at a constant working pressure of 0.3 Pa. Film thicknesses were determined on alpha-step 500 apparatus. The deposition rate was approximately 2.06 nm/min. All the samples with different thicknesses were prepared under identical deposition condition. These Ag films thicknesses are 5, 8.24, 17.51, 26.78, 41.2, 51.5, and 107.2 nm, respectively. All the investigated samples mentioned below are nominated as samples 1—7.

Optical spectra in the wavelength range from 420 to 680 nm were measured for each deposited film at near normal incidence on a Perkin-Elmer Lambda 900 spectrophotometer, which were applied in the following section for known thickness to accurately calculate effective film optical constants. The scattering and roughness were obtained on the total integrated scattering (TIS) instrument. The crystalline structure of the films was

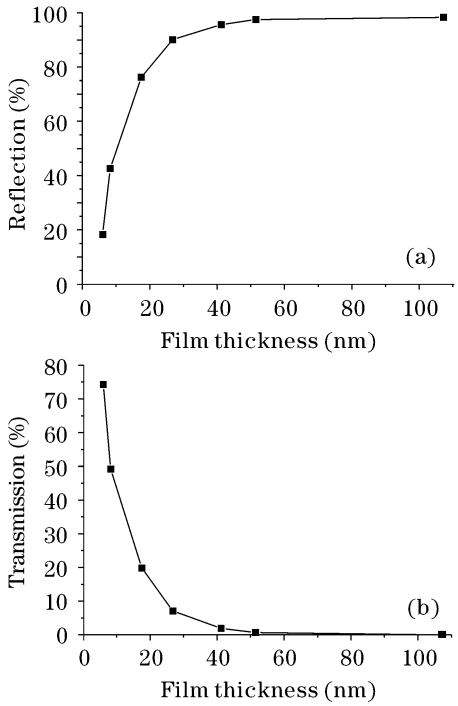

Fig. 2. Reflection and transmission spectra from Ag film as a function of film thickness.

characterized by grazing angle X-ray diffraction (XRD) using Cu $K\alpha$ radiation and an incidence angle $10^\circ - 90^\circ$ with a step width of 0.02°.

Both the reflection (R) and transmission (T) spectra of the Ag film at 633-nm wavelength are function of film thickness between 5 and 107 nm, as shown in Fig. 2. The reflection rapidly increases to 76% as the Ag film increases to around 17.5 nm, and then increases slowly in the range of thickness interval from 17.5 to 41 nm, and tends to be stable when the thickness is over 41 nm. The transmission varies inversely. It decreases rapidly below 17.5 nm, and then decreases slowly between 17.5 and 41 nm, and tends to zero above 41 nm. The variation may correspond with the growth mode of silver film. Below the critical thickness, the area occupied by Ag particles increases quickly with film thickness. When the film thickness increases above the critical thickness, the area occupation increases slowly and a closed film with no voids is formed gradually[12]. So the optical properties of the Ag film tend to be stable. It can be deduced that the reflection and transmission may have a saturation value with increasing film thickness.

The optical constants given here were obtained from reflectance and transmittance for unpolarized light at near normal incidence using the computer program with Newton methods, in which the initial estimates of refractive index and extinction coefficient should be close to the correct values in order to give convergence of the iteration. Figure 3 shows the dependence of complex

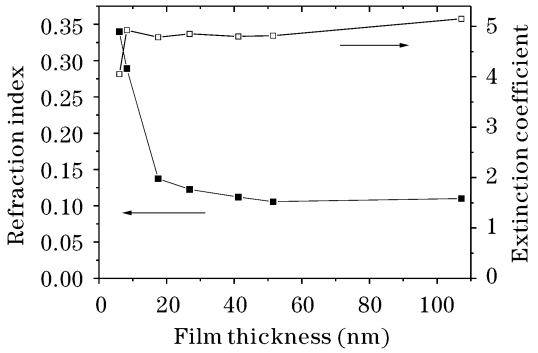

Fig. 3. Complex refractive index of Ag film as a function of film thickness.

refractive index at 633-nm wavelength on the Ag film thickness.

The refractive index decreases with the film thickness increasing. Above a thickness of 17.5 nm it tends to be stable. The variation, which can be explained by the Bruggman's effective medium theory (EMT)[13], correlates with the film growth. The grains sizes and some residual voids significantly affect the effective optical constants. During the initial deposition stage the Ag island films were formed on the substrates, and the area fraction occupied by the metal particles was small. There were many voids in the stage. With further deposition, the area fraction rises rapidly and the refractive index decreases quickly. Then the islands are linked and form continuous films with no voids where there is no obvious change in the microstructure, so the refractive index tends to be a constant level.

There is a peak at the thickness of around 8 nm in the plot of the extinction coefficient variation with the film thickness. Below 8 nm the extinction coefficient rises with increasing thickness, and then drops to be stable till 51.5 nm. However, the extinction coefficient value of 107-nm film thickness has a rise, which may be due to the part oxidation of Ag film. The peak appeared in the plot can be explained by the interband transitions of the bound electrons. When the film thickness is comparable to the quantum size, the discreteness of the energy levels resulting from the geometrical quantization plays an important role. The outer shell electronic structure of Ag is $4d^{10}5s^1$ and the $4d$ and $5s$ energy levels are near the Fermi level. It is quite possible that the bound $4d$ electrons transit to the Fermi level or the electrons at the Fermi level transit to the $5s$ level, causing the appearance of a peak in the extinction coefficient[7].

In the experiment, the refractive index and the extinction coefficient agree well with the data from Ref. [14] at the thickness when a continuous film is formed.

The surface scattering and the root mean square (RMS) roughness are shown in Table 1. It can be seen that the surface scattering losses increase to a maximum

Table 1. Surface Scattering and Root Mean Square Roughness (RMS) of the Sample Measured on the TIS Instrument

Film Thickness (nm)	5	8.24	17.51	26.78	41.2	51.5	107.2
RMS (nm)	0.64	0.77	0.53	0.51	0.5	0.49	0.49
Surface Scattering ($\times 10^{-4}$)	1.61	2.34	1.11	1.02	0.98	0.95	0.95

and then decrease to a constant value with increasing film thickness. It has been shown that most metal films grow from initially isolated metallic islands to a connecting network and finally to complete coverage of the whole area. When the film thickness is small, the metallic film consists of isolated metallic particles. So light passing through the film is scattered a lot. The particle size increases as thickness increases. When the metallic film reaches a certain thickness, the metal particles have coalesced to form short chain of irregular length and shape. When thickness further increases, it is possible to see connecting paths across a large area of the film and form continuous film. Now the crystal boundaries decrease and the scattering decreases[12].

From Table 1, the scattering losses change by 10^{-4} or 10^{-5} orders of magnitude. So we assume the sputtered Ag films have effective homogenized optical properties and the absorption of Ag films $A = 1 - R - T$. The absorption value versus film thickness is plotted in Fig. 4. With increasing film thickness, the absorption value rises to a peak and then drops gradually, which corresponds to the scattering variation and can be explained with different growth modes of Ag films. The optical properties of aggregated metal films differ considerably from closed films, they show a much higher absorption than the closed films.

The maximum absorption value coincides with the percolation threshold[15]. Below the percolation threshold, there are many voids along the substrate and the electrons are trapped in isolated islands, which induced the surface plasmon resonance when light waves were incident on the silver films, thus result in high absorption. At the percolation threshold, the largest amount of Ag atoms is trapped in individual islands, corresponding to the highest absorption. With increasing deposition, the isolated islands are connected and the electrons can move freely. This reduces the probability of the excitation of surface plasmon and thus the absorption.

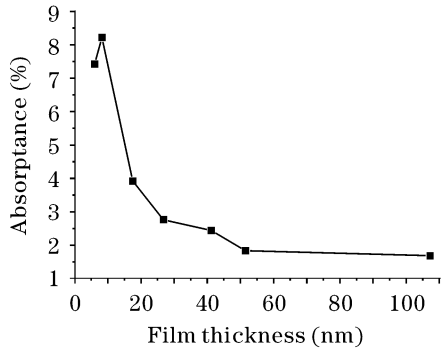

Fig. 4. Absorption spectrum of Ag film as a function of film thickness.

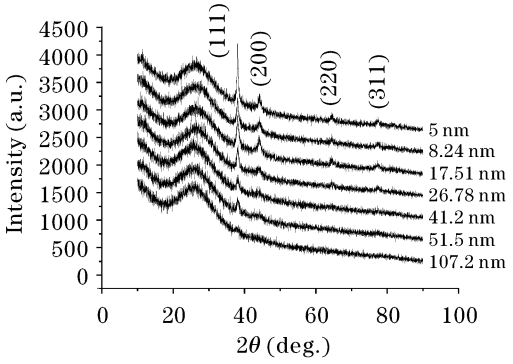

Fig. 5. XRD spectra of Ag films with different thicknesses.

XRD spectra as shown in Fig. 5 reveal the influence of film thickness on the structure of the thin Ag films. It can be seen that the crystalline quality and texture of all the Ag samples are very similar. There are all fcc-Ag grains and four diffraction peaks appeared in the spectra, namely the (111), (200), (220) and (311) peaks. The low angle (111) Ag peak is the most intense in the pattern, which implies a light preferential orientation of the Ag grains along the (111) crystallographic direction. The (111) direction in Ag film has the lowest surface energy[16], therefore equilibrium growth conditions lead to a (111) orientation. Nonequilibrium conditions give rise to other grain orientations, which are detected as other XRD peaks such as (200), (220), and (311). The Ag (111) orientation peak is very weak when the film is thin and does not absorb all the incident radiation, so do the high angle peaks. Compared with the Ag powder (the interplanar spacing of (111) orientation d_{111} is 0.2359 nm), all the films formed in our experiment exhibit discrepancy in d-value and are all larger than the Ag powder, which is due to the variation of residual stresses in the films. The peak positions are 38.086°, 38.098°, 38.131°, 38.133°, and 38.153°, respectively. The full-width at half-maximum (FWHM) are 0.802°, 0.798°, 0.777°, 0.742°, and 0.736°, respectively. It is evident that as the film thickness increases, there is a shift of (111) diffraction peaks to higher angles and a reduction of the FWHM, which indicates that grain growth has occurred and results in the partial relief of intrinsic stress within the films. From the FWHM and peak position of the (111) peak, the grain size and the film stress are calculated. It shows that the grain sizes and the film stresses are related to the film thickness. With increasing the thickness, the absolute peak intensities increase and peak widths reduce, which suggesting an increase in the fraction of crystalline Ag. The grain sizes in Ag films were calculated according to the Scherrer formula: $D = 0.09\frac{\lambda}{\beta \cos \vartheta}$, where λ is the X-ray wavelength (λ = 0.154186 nm), β is FWHM of the (111) reflection as a function of 2θ, θ is the incident angle of the X-ray measured for the sample surface and ϑ is the Bragg angle. The interplanar spacing d can be evaluated from the relation: $2d \sin \vartheta = \lambda_{\mathrm{Cu}K\alpha}$. The calculated results are shown in Table 2.

Large residual stresses are commonly found in sputtering films. Since the deposition temperature is at room temperature, the main residual stresses are the intrinsic stresses arising from the film density and structure. From above, the residual stresses exhibit compressive, and reduce from 587.56, 566.84, 508.38, 485.44 to 457.32 MPa with increasing thickness. It is proposed that the compressive intrinsic stresses provide a driving force for the grain growth during the increasing film thickness. The compressive film stress arises from a high atomic packing density and frozen-in crystallographic defects in the grains and boundaries[16]. Since the intragranular defects and grain boundaries contain more free energy than crystalline phase, the increase of the grain size in

Table 2. FWHM, Average Grain Size and Interplanar Spacing Evaluated from XRD θ-2θ Scans for the Samples

Sample	Thickness (nm)	FWHM (deg.)	Stress (MPa)	Average Grain Size (nm)	Interplanar Spacing (nm)
3	17.51	0.802	−587.56	10.094	0.4007
4	26.78	0.798	−566.84	10.157	0.3888
5	41.2	0.777	−508.38	10.467	0.3595
6	51.5	0.742	−485.44	10.961	0.3578
7	107.2	0.736	−457.32	11.078	0.3423

the films lowers free energy with increasing the film thickness.

In this work, the dependence of optical properties and microstructure of Ag films on the film thickness is investigated. The results show that the optical properties, such as reflection, transmission, absorption, and microstructure change as Ag film grows. It is also found that the optical constants of Ag film vary obviously with increasing the film thickness below the percolation threshold and then tend to be stable when a closed film is formed. And the reasonable explanation is given.

X. Sun's e-mail address is xiliansun@siom.ac.cn.

References

1. A. Rizzo, M. A. Tagliente, M. Alvisi, and S. Scaglione, Thin Solid Films **396,** 29 (2001).
2. C. Charton and M. Fahland, Surf. Coat. Technol. **142—144,** 175 (2001).
3. S. M. A. Durrani, E. E. Khawaja, A. M. Al-Shukri, and M. F. Al-Kuhaili, Energy and Buildings **36,** 891 (2004).
4. G. Leftheriotis, S. Papaefthimiou, and P. Yianoulis, Solid State Ionics **136—137,** 655 (2000).
5. E. Bertran, C. Corbella, M. Vives, A. Pinyol, C. Person, and I. Porgueras, Solid State Ionics **165,** 139 (2003).
6. Z. Wang, Q. Chen, and X. Cai, Appl. Surf. Sci. **239,** 262 (2005).
7. J.-J. Xu and J.-F. Tang, Appl. Opt. **28,** 2925 (1989).
8. H. H. Hurt and J. M. Bennett, Appl. Opt. **24,** 2712 (1985).
9. M. H. Lee, P. J. Dobson, and B. Cantor, Thin Solid Films **219,** 199 (1992).
10. R. R. Singer, A. Leitner, and F. R. Aussenegg, J. Opt. Soc. Am. B **12,** 220 (1995).
11. N. Mayani, F. Varnier, and G. Rasigni, J. Opt. Soc. Am. A **7,** 191 (1990).
12. P. Fan, J.-D. Shao, K. Yi, H.-J. Qi, and Z.-X. Fan, Chin. J. Lasers (in Chinese) **32,** 977 (2005).
13. D. E. Aspnes, E. Kinsbron, and D. D. Bacon, Phys. Rev. B **21,** 3290 (1980).
14. P. B. Johnson and R. W. Christy, Phys. Rev. B **6,** 4370 (1972).
15. C. Charton and M. Fahland, Surf. Coat. Technol. **174—175,** 181 (2003).
16. Y. Zeng, Y. L. Zou, and T. L. Alford, J. Appl. Phys. **81,** 7773 (1997).